An Eco-Routing Algorithm for HEVs Under Traffic Conditions

Arthur Le Rhun, Frédéric Bonnans, Giovanni De Nunzio, Thomas Leroy, Pierre Martinon

Available online at www.sciencedirect.com

ScienceDirect

IFAC PapersOnline CONFERENCE PAPER ARCHIVE

IFAC PapersOnLine 53-2 (2020) 14242–14247

An Eco-Routing Algorithm for HEVs Under Traffic Conditions

Arthur Le Rhun * **Frédéric Bonnans** * **Giovanni De Nunzio** ** **Thomas Leroy** ** **Pierre Martinon** ***

* *A. Le Rhun and F. Bonnans are with Inria Saclay and CMAP Ecole Polytechnique, route de Saclay, 91128 Palaiseau, France,* [arthur.le-rhun, frederic.bonnans]@inria.fr

** *G. De Nunzio and T. Leroy are with IFP Energies nouvelles, 1 et 4 avenue de Bois-Préau, 92852 Rueil-Malmaison, France,* [giovanni.de-nunzio, t.leroy]@ifpen.fr

*** *P. Martinon is with Inria Paris and Sorbonne-Université, CNRS, Université de Paris, Laboratoire Jacques-Louis Lions (LJLL), F-75005 Paris, France,* pierre.martinon@inria.fr

Abstract:
In a previous work, a bi-level optimization approach was presented for the energy management of Hybrid Electric Vehicles (HEVs), using a statistical model for traffic conditions. The present work is an extension of this framework to the eco-routing problem. The optimal trajectory is computed as the shortest path on a weighted graph whose nodes are (position, state of charge) pairs for the vehicle. The edge costs are provided by cost maps from an offline optimization at the lower level of small road segments. The error due to the discretization of the state of charge is proven to be linear if the cost maps are Lipschitz. The classical A^* algorithm is used to solve the problem, with a heuristic based on a lower bound of the energy needed to complete the travel. The eco-routing method is compared to the fastest-path strategy by numerical simulations on a simple synthetic road network.

Keywords: Eco-routing, bi-level optimization, traffic model

1. INTRODUCTION

Road networks usually allow several paths to reach a destination given a starting position. While paths are traditionally chosen to minimize travel time, methods to minimize the fuel consumption have received increased attention in the recent years. This new criterion gives rise to the so-called eco-routing problem. The fuel savings between the optimized eco-routing and the path naturally chosen by the drivers can be important, up to 25% Ahn and Rakha (2007); Ericsson et al. (2006). Besides, distance minimal paths have been shown to differ from the eco-routing paths, especially in congested traffic Barth et al. (2007). This indicates that eco-routing planning needs to take into account the traffic conditions.

Most methods propose to solve the eco-routing planning based on shortest path algorithms, using weighted graphs to represent the road network with edge costs corresponding to the consumption, see De Nunzio et al. (2017). Dijkstra or A^* algorithms can be used when edge costs are positive, or the slower Ford-Bellman algorithm when edge costs can be negative Bellman (1958).

In the case of HEVs, expressing the costs in terms of fuel consumption instead of energy gives positive costs, but requires knowledge of the torque policy of the vehicle. Consumption estimators, that take traffic conditions into account, are usually divided in two main categories: macroscopic models based on closed algebraic forms Lighthill and Whitham (1955), and microscopic models based on differential equations Panwai and Dia (2005).

The main contribution of the present work is to adapt the bi-level approach from Le Rhun et al. (2019a), which handles traffic conditions in a statistical way, with the vehicle following probability distributions for speed and acceleration. More precisely, the method was previously used to optimize a single known travel, while we now tackle the eco-routing problem of finding the optimal path on a given road network.

The paper is organized as follows. Section 2 introduces the models for the hybrid vehicle, traffic conditions, and states the eco-routing problem of HEVs resulting from the bi-level decomposition. Section 3 details the numerical errors due to the discretization. Section 4 presents the complexity of the algorithm used to solve the eco-routing problem. Section 5 discusses the numerical simulations performed using actual traffic data, mapped to a small synthetic road network.

2. MODELING APPROACH

2.1 Vehicle model

Let us consider an HEV with 'parallel' design (see e.g. Chau and Wong (2002)), where both the thermal engine

10.1016/j.ifacol.2020.12.1158

and the electric motor can power the vehicle. Such HEVs can use the engine to recharge the battery, which allows for optimization of the global consumption along the travel.

Neglecting losses due to mechanical links, the torque of the engine T_e and motor T_m are linked through:

$$T_{prim}(v,a) = T_e + T_m R \tag{1}$$

with the expression of the torque at the primary shaft $T_{prim}(v,a)$ described in Appendix A, and R the reduction ratio between the engine and the motor.

Through experimental characterization, the consumption of the engine is modeled as a map $\hat{C}(\omega_e, T_e)$ depending on the rotation speed and torque request. The model presented in Appendix A is used to reformulate the consumption as a function of the electric motor torque T_m, i.e.

$$C(v,a,T_m) = \hat{C}(\omega_e(v,a), T_{prim}(v,a) - T_m R) \tag{2}$$

Likewise, consider a map for the electrical power $\hat{P}_m$ required by the motor:

$$P_m(v,a,T_m) := \hat{P}_m(\omega_m(v,a), T_m), \tag{3}$$

with the convention that $P_m > 0$ for a discharge. Denoting C_{max} the maximum capacity of the battery and $SoC(t) \in [0,1]$ its state of charge at time t, the dynamics of the state of charge then writes as:

$$\dot{SoC}(t) = \frac{1}{C_{max}} P_m(v(t), a(t), T_m(t)). \tag{4}$$

2.2 Road network model with traffic conditions

The consumption of a vehicle on a given portion of road is influenced by many parameters, that can be static such as the speed limit or the slope, or transient such as traffic and weather conditions. In the following, the road network is modeled as a graph where roads are the edges and intersections the nodes. The characteristics of the road portions are then attributes of the edges. In the present work these attributes also include the traffic conditions, modeled as probability laws.

We use here the probabilistic traffic model introduced in Le Rhun et al. (2019b). The model is based on a subdivision of the roads into small *segments*, typically delimited by topological characteristics. We assume that the speed and acceleration of the vehicles on each segment are random variables $(\mathbf{V}(t), \mathbf{A}(t))$, constant over each time step $h_0 > 0$, with discrete independent and identically distributed (i.i.d.) distributions μ^s, called the *traffic distribution*. Fig. 1 shows an example of such a distribution.

We make the central assumption that drivers 'follow the traffic', meaning that their speed and acceleration coincide with the random variables $(\mathbf{V}(t), \mathbf{A}(t))$. Le Rhun et al. (2019b) established that this traffic model provides a statistically accurate estimate of the energy consumption of the hybrid vehicle.

The state graph for hybrid electrical vehicles In the case of internal combustion engine (ICE) vehicles, the optimal path, i.e. the successive positions of the vehicle on the road graph, is sufficient to define the optimal strategy. In the case of a hybrid vehicle, the energy stored in the battery can be used to reduce the fuel consumption, adding a supplementary state, the state of charge (SoC) of the battery. Therefore the optimal consumption policy consists of the successive vehicle positions and states of charge of the battery.

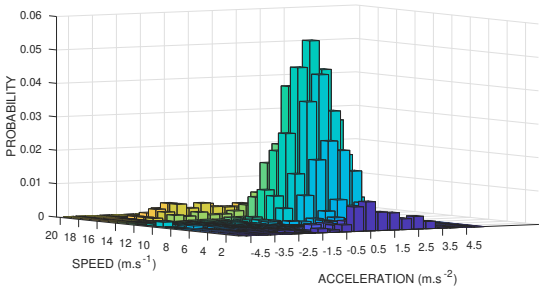

Fig. 1. Illustrative example of (speed,acceleration) distribution obtained from the traffic simulator SUMO.

Using the lexicographic product between graphs, see Fig. 2, we define the 'state graph', denoted Γ, whose nodes have a form (N, SoC), with N a node of the road graph and SoC is a non-empty discrete set of state of charges values. Therefore an edge between (N_1, SoC_1) and (N_2, SoC_2) exists if and only if there is an edge between N_1 and N_2.

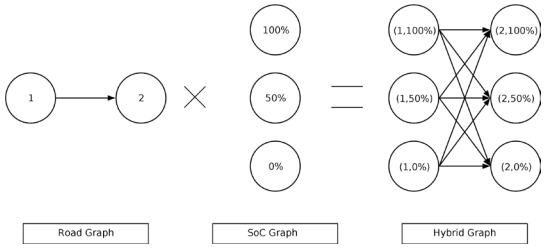

Fig. 2. Illustration of the lexicographic product

Finding the optimal path on the 'state graph' provides an approximation of the solution of the eco-routing problem for HEV.

Cost of an edge Since the consumption of the vehicle depends on the road and the traffic conditions, each edge has a specific expected cost. In order to obtain the edge cost $\nu_{NN'}(SoC, SoC')$ between two nodes (N, SoC) and (N', SoC'), the method proposed in Le Rhun et al. (2019a) is used. Namely, the expected consumption on the road segment $s_{NN'}$, with (SoC, SoC') as initial and final SoC conditions, is taken as the value of the following optimization problem, denoted as $\mathcal{P}^{s_{NN'}}_{micro}$:

$$\min_{T_m} \ \mathbb{E}\left[\int_{t=0}^{t_f} C(\mathbf{V}(t), \mathbf{A}(t), T_m(t))\mathrm{d}t + P_{s_{NN'}}(SoC_{s_{NN'}}(t_f), SoC')\right] \tag{5}$$

$$s.c\ \forall t,\ \dot{SoC}_{s_{NN'}}(t) = \frac{1}{C_{max}} P_m(\mathbf{V}(t), \mathbf{A}(t), T_m(t)) \tag{6}$$

$$\dot{D}_{s_{NN'}}(t) = \mathbf{V}(t) \tag{7}$$

$$T_m(t) \in [T_{min}, T_{max}] \tag{8}$$

$$SoC_{s_{NN'}}(t) \in [0,1] \tag{9}$$

$$SoC_{s_{NN'}}(0) = SoC,\ D_{s_{NN'}}(0) = 0 \tag{10}$$

$$t_f = \min\{t, D_{s_{NN'}}(t) > L_{s_{NN'}}\} \tag{11}$$

where $L_{s_{NN'}}$ denotes the length of the segment and $D_{s_{NN'}}$ the traveled distance on it.

2.3 Optimal path for HEV under traffic conditions

It is now possible to formulate an eco-routing problem for HEV as finding the optimal path on the 'state graph' Γ between a start node S and a destination node D. We denote by Γ_{SD} the set of paths between S and D in the 'state graph', with γ denoting a single path. This optimal path problem consists in finding a target state of charge trajectory SoC^r. We introduce a_i (resp. b_i) the maximum charge (resp. discharge) to reduce the search space. Setting $a_i = 1$ and $b_i = 1$ restores the original discrete problem. The choice of a_i (resp. b_i) can be guided by the vehicle and segment characteristics. In the sequel, we assume:

$$a_i > 0, b_i > 0 \tag{12}$$

Therefore the eco-routing problem can be stated as follows:

$$\begin{aligned} \underset{\gamma\in\Gamma_{SD}}{\text{minimize}} \quad & \sum_{i\in\gamma} \nu_{N_iN_{i+1}}(SoC_i^r, SoC_{i+1}^r) && (13)\\ \text{s.t} \quad & \forall i \in \gamma, SoC_i^r \in [0,1] && (14)\\ & \forall i \in \gamma,\ SoC_{i+1}^r - SoC_i^r \in [-a_i, b_i] && (15) \end{aligned}$$

3. DISCRETIZATION ERROR ANALYSIS

Since the SoC is discretized, it is useful to analyze the error between the discrete problem (P_h) and the continuous one (P) defined below. Indeed, let be a path γ on the road network, and consider the consumption minimization problem on this path. Let us define the criterion:

$$F^\gamma(SoC^r) := \sum_{i\in\gamma} \nu_{N_iN_{i+1}}(SoC_i^r, SoC_{i+1}^r) \tag{16}$$

Denote the continuous problem by (P^γ), and the discrete problem by (P_h^γ).

$$\begin{aligned} \underset{SoC^r}{\text{minimize}} \quad & F^\gamma(SoC^r) && \\ \text{s.t} \quad & \forall i \in \gamma, SoC_i^r \in [0,1] && (P^\gamma)\\ & \forall i \in \gamma, SoC_{i+1}^r - SoC_i^r \in [-a_i, b_i] && \\ \underset{SoC^r}{\text{minimize}} \quad & F^\gamma(SoC^r) && \\ \text{s.t} \quad & \forall i \in \gamma, SoC_i^r \in \{0, h, ..., 1\} && (P_h^\gamma)\\ & \forall i \in \gamma, SoC_{i+1}^r - SoC_i^r \in [-a_i, b_i] && \end{aligned}$$

Denote the value of (P_h^γ) by V_h^γ, and the value of (P^γ) by V^γ. Let the eco-routing problem (P) be

$$\min_\gamma(V^\gamma) \tag{P}$$

and its discrete approximation (P_h) be

$$\min_\gamma(V_h^\gamma). \tag{P_h}$$

Theorem 1. Discretization Error

Assume that the criterion F^γ is Lipschitz continuous with constant L. Let S^* be a solution of (P^γ). Then there exists S_h feasible for (P_h^γ), such that $|S_h - S^*| = O(h)$ and

$$F^\gamma(S^*) \le F^\gamma(S_h) \le F^\gamma(S^*) + O(h). \tag{17}$$

Proof. Let S^* be an admissible solution for (P^γ). Set $\hat{S} := (1-\varepsilon)S^*$. Then $\hat{S} \in [0,1]$ and also

$$\hat{S}_{i+1} - \hat{S}_i \ \in [-(1-\varepsilon)a_i, (1-\varepsilon)b_i].$$

Define the discretized grid $H = \{0, h, ..., 1\}$, and a projector Π_h over H such that

$$\Pi_h(x) \in \underset{h\in H}{\text{argmin}}(|x-h|) \tag{18}$$

Let $\hat{S^h} := \Pi_h(\hat{S})$. Then $\hat{S^h} \in \{0, h, ..., 1\}$ and

$$\hat{S}_{i+1} - \hat{S}_i \in [-(1-\varepsilon)a_i - h, (1-\varepsilon)b_i + h]. \tag{19}$$

Therefore $\hat{S}_h$ is feasible for problem (P_h^γ) if and only if:

$$h - \varepsilon b_i \le 0 \quad , \quad \varepsilon a_i - h \ge 0 \tag{20}$$

Thanks to assumption (12), we can take:

$$\varepsilon = \frac{h}{\min(\min_i(a_i), \min_i(b_i))} \tag{21}$$

Therefore, $\varepsilon = O(h)$. An admissible solution of (P_h^γ) is at $O(h)$ distance of an admissible solution of (P^γ). Since the objective function F^γ is Lipschitz continuous, the conclusion follows.

Corollary 2. Under the hypothesis of Theorem 1, we have that

$$\text{val}(P) \le \text{val}(P_h) \le \text{val}(P) + O(h) \tag{22}$$

4. ROUTING ALGORITHM

The class of problems under consideration has directed graphs and non-negative costs. Therefore, we may use the classical Dijkstra's algorithm, see for instance Cormen (2009). Another possibility is to use the A^* algorithm, a generalization of Dijkstra's algorithm based on a heuristic estimate (called the heuristic distance) H of the distance of nodes to the destination node, allowing to decrease the number of visited nodes.

The A^* algorithm computes the optimal path if the heuristic distance H is *admissible* in the sense below, see Nilsson (1980).

Definition 3. Admissibility

A heuristic H is admissible if it never overestimates the real cost to reach the goal. In other terms,

$$\forall v \in \Gamma, H(v) \le H^*(v) \tag{23}$$

where $H^*(v)$ is the minimum cost between node v and the goal node.

4.1 Complexity

The complexity of the A^* algorithm has been discussed for instance in Martelli (1977). In the worst-case scenario, the destination node is explored after all the other nodes on the graph, and after that all the edges have been explored too. If n is the number of nodes and m the number of edges, the complexity is $O(n * operations + m * operations)$. The only operation which is not in $O(1)$ is the minimization over the nodes, that can be made in $O(log(n))$. Then the complexity is $O(n * \log(n) + m)$ and we have that $m \le n^2$. So the complexity of the A^* algorithm in the worst possible case is $O(n^2)$.

However, the number of nodes of the state graph depends of the discretization on the SoC^r as well as the number

of edges. The number of nodes of the state graph is the product of the number of intersections n in the road network and the number of SoC divisions created. The number of edges of the state becomes m/h^2. Then the complexity of the A^* algorithm according to the problem is $O(n/h \log(n/h) + m/h^2)$.

4.2 Heuristic distance

We propose here an admissible heuristic for the case of the hybrid vehicle eco-routing. Define H_c an estimate of the consumption to reach the physical destination

$$H_c := \eta_m \alpha_0 L \tag{24}$$

with L the travel length, η_m the maximum efficiency of the ICE to convert fuel to mechanical energy, α_0 defined in Appendix A.

Similarly, define H_{SoC} as an estimate of the consumption to reach the desired state of charge

$$H_{SoC} := \eta_e C_{max}(SoC_f - SoC_{current}) \tag{25}$$

with η_e the maximum efficiency of the ICE to convert fuel to battery charge.

Finally, to take into account the possibility of regenerative braking that can recover the kinetic energy of vehicle, let us define $H_{kinetic}$

$$H_{kinetic} := \frac{\eta_c m}{2} v_{max}^2 \tag{26}$$

with η_c a conversion factor of the kinetic energy into fuel according to the ICE and v_{max} the maximum speed. Since the aim is to reach a specific destination with a final state of charge, the heuristic is taken as the sum of these estimates. Additionally, taking into account that the fuel cannot be produced by the vehicle, the final expression is:

$$H := \max(0, H_c + H_{SoC} - H_{kinetic}) \tag{27}$$

5. NUMERICAL SIMULATIONS

We now present numerical simulations for the eco-routing method. Consider a simple road network comprised of a small ring with congested traffic with a mean speed of 40 km/h, enclosed in a larger ring with fluid traffic with a mean speed of 100 km/h. This can be considered as a very simplified model of a typical road network with ring roads around a city. For the sake of simplicity, each segment of the presented network has the same topological aspects. In particular, we are interested in comparing the solution from the eco-routing, called 'eco-path' in the following, with the fastest path. We first study a specific travel with a fixed origin and destination, and then give some more general results on all possible travels in the network.

5.1 Study of a single travel

Fig. 3 shows the eco-path (green, left graph) and fastest path (orange, right graph) for a given travel with conditions ($SoC_i = 30\%, SoC_f = 25\%$). Note that the considered vehicle has a low battery capacity, see C_{max} in Table A.1, allowing for relatively significant SoC changes even on small road segments. The SoC values at the end of each road segment are indicated on the nodes, while the values of the objective function in (5) of the problems $\mathcal{P}_{micro}^{s_{NN'}}$ are displayed along each edge. In this particular example, the

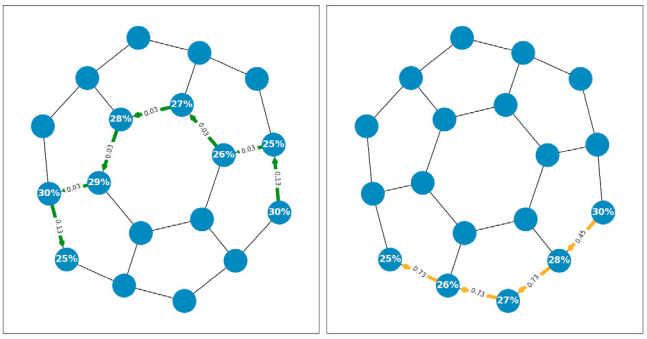

Fig. 3. Eco-path (left) and Fastest Path (right) - ($SoC_i = 30\%, SoC_f = 25\%$)

fastest path takes the 4 fast segments on the outer ring, while the eco-path uses the slower inner segments to reduce the consumption, with 7 segments in total.

Path	Value	Cons. (l)	SoC_f (%)	Time (s)	Dist. (km)
Eco	0.41	0.012	21	163	2.14
Fastest	2.66	0.038	4	44	1.22

Table 1. Comparison of Eco and Fastest Path - ($SoC_i = 30\%, SoC_f = 25\%$).

Table 1 summarizes for both paths the sum of values of the objective function in (5), consumption, final SoC, time and distance for a $SoC_f = 25\%$ constraints. The time is based on the average speed of each segment. The consumption and final SoC are calculated by taking the average of 1000 travels simulated with i.i.d. sampling according to the traffic conditions and using the local optimal policies determined by the eco-path. For this sample travel the eco-path consumption is one third of the fastest path, for a double distance and four times longer time. Note that the difference in terms of value is greater than the difference in consumption, which indicates that the eco-path has a better chance of following the reference SoC trajectory, since the value function of $\mathcal{P}_{micro}^{s_{NN'}}$ is the sum of the consumption and penalty for the final SoC constraint at the end of the segment. This also shows in the final SoC value, with the eco-path being much closer to the prescribed $SoC_f = 25\%$, reaching 21% while the fastest path ends up at only 4%.

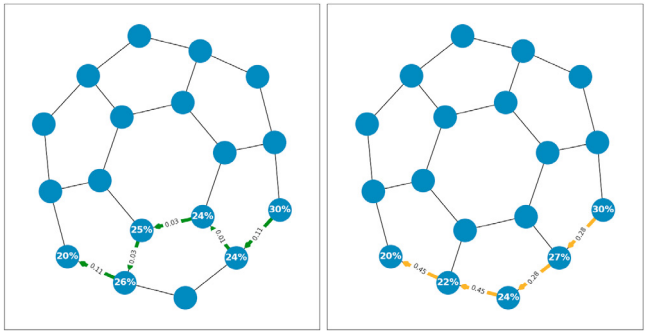

Fig. 4. Eco-path (left) and Fastest Path (right) - ($SoC_i = 30\%, SoC_f = 20\%$)

Fig. 4 and Table 2 show the same results for a final constraint $SoC_f = 20\%$. The consumption is still one third of the one of the fastest path, but now with a more

Path	Value	Cons. (l)	SoC_f (%)	Time (s)	Dist. (km)
Eco	0.28	0.013	19.7	106	1.53
Fastest	1.46	0.036	4	44	1.22

Table 2. Comparison of Eco and Fastest Path - ($SoC_i = 30\%, SoC_f = 20\%$).

moderate increase in travel distance and time. Also notice that the final SoC constraint is well satisfied in this case by the eco-path, reducing the gap between the i.i.d.-simulated consumption and the value of the eco-routing problem. All in all, a classical trade-off is observed, with the eco-routing having a lower consumption and better management of the state of charge, at the expense of choosing longer and slower paths.

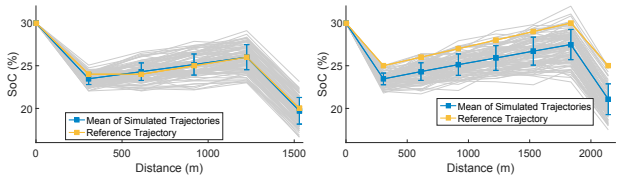

Fig. 5. Simulated and reference SoC trajectories for $\Delta SoC = -10\%$ (left) and $\Delta SoC = -5\%$ (right). Markers show the mean and vertical bars show $\pm\sigma$ of the simulated trajectories.

Now, let us study the SoC a bit more in detail, with Fig. 5 showing the evolution of the state of charge along the travel. Orange line is the reference SoC from the eco-routing solution, while blue line is the average (with standard deviation indicators) of the 1000 i.i.d simulations, with the first 100 simulations also plotted in grey lines. For the condition $\Delta SoC = -10\%$ (left), the reference SoC is very well matched by the set of simulations, which means that the control decisions from the problems $\mathcal{P}_{micro}^{s_{NN'}}$ are able to satisfy the individual final SoC constraints at the end of each segment. In this case the penalty terms are typically close to zero, and the value function is close to the consumption. For the stricter condition $\Delta SoC = -5\%$ (right), the $\mathcal{P}_{micro}^{s_{NN'}}$ solutions begin to have difficulties to reach the required SoC, which leads to penalty terms in the value function (as seen in Table 1 and Table 2) and a growing gap between the reference SoC from the eco-path and the actual SoC trajectory from the simulated travels.

In order to look a bit more into the influence of the final SoC condition, we solve the previous test case for ΔSoC ranging from -10% to $+5\%$. We compare in particular the final SoC and consumption for the eco-path and the simulated trajectories. Fig. 6 shows the final SoC (eco-path reference and simulations average with std indicators). The reference final SoC basically corresponds to the ΔSoC constraint (recall that $SoC_i = 30\%$). As for the simulated SoC, for easier constraints such as 10% discharge, it coincides well with the reference, as already seen above in Fig. 5. When the final SoC condition tightens, the gap between the two curves increases, due to the fact that some of the $\mathcal{P}_{micro}^{s_{NN'}}$ solutions selected for the eco-path do not satisfy their prescribed SoCs. A way to reduce these gaps could be to use a smaller discretization for the initial and final SoC of the $\mathcal{P}_{micro}^{s_{NN'}}$ problems, enabling the routing algorithm to choose reference SoCs closer to the maximum feasible ΔSoC on the segments. Note also that for sufficiently long travels with more opportunities for recharging the battery, the gap may be compensated along the way, see the simulations of Le Rhun et al. (2019a).

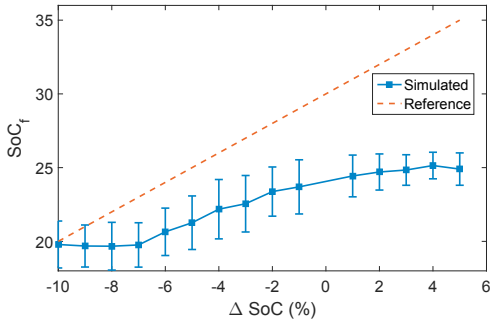

Fig. 6. Reference and simulated SoC_f

Fig. 7 shows the simulated consumption for the eco and fastest paths. We observe a clear advantage of the eco-paths overall, with a consumption between one quarter and one third of the fastest path. The consumption for the fastest path tends to increase with respect to the ΔSoC, since the harder final SoC constraint requires an additional use of the engine. On the other hand, the consumption of the eco-path appears non-increasing, which is probably explained by the fact that the eco-path maintains a low consumption at the expense of an increasing violation of the final SoC constraints, see Fig. 6. This is related to the fact that the $\mathcal{P}_{micro}^{s_{NN'}}$ problems manage the reference SoC constraints thanks to the penalization term, which allows some trade-off between the consumption and the reference SoC constraints.

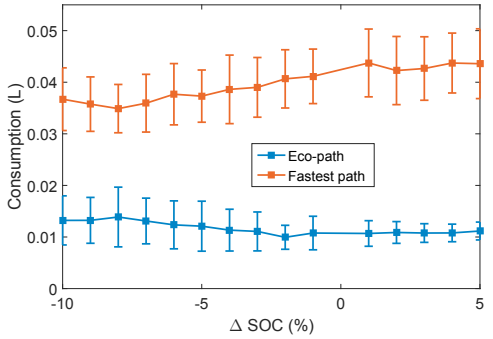

Fig. 7. Eco-path and fastest path consumption

5.2 Study of all possible travels

Previous simulations focused on a single travel, and we now perform some simulations while taking into account all possible travels on the road graph. The symmetry of the road network leads to a set of 54 travels that are solved for varying final SoC conditions. Fig. 8 shows the average time and distance ratio between the eco-path and the fastest path (i.e. the average of the ratios for each individual travel).

For harder final SoC constraints, there is a large difference between the two paths, with the eco-path being (on average) up to 7 times slower and 4 times longer than the fastest path. This behavior comes from the eco-path traveling repeatedly along segments that allow for recharging

the battery, in order to meet the final constraint of a 5% charge. Note that this type of path seems to include cycles in the 'physical' road graph, but these are not cycles in the weighted graph augmented with the SoC values.

When the final SoC constraints are easier to meet, the average time and distance of the eco-path and fastest path tend to be closer. Indeed, allowing an increased discharge of the battery will reduce the consumption of the fastest path, up to the point that it actually becomes identical to the eco-path.

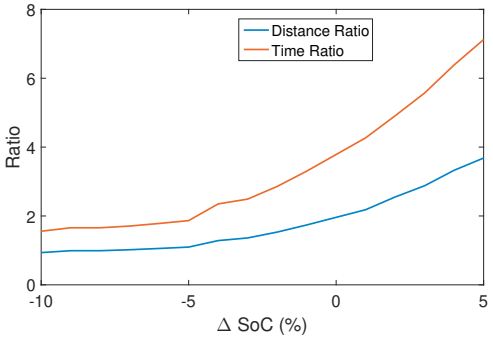

Fig. 8. Time and Distance Ratio

6. CONCLUSION

Simulations on a simple road network indicate that the eco-routing method computes optimal paths with a consumption significantly lower than the fastest path solutions. This reduced consumption comes with an expected trade-off in terms of travel distance and time. Considering an upper bound for time and/or distance would be a natural extension of the method, in order to obtain solutions that can fit the expectations of the drivers. Also, the accuracy of the reference SoC trajectory computed by the eco-routing tends to decrease for stricter final SoC conditions. Increasing the weight of the penalty term for the final SoC constraint would also improve this accuracy, however at the expense of a higher consumption overall. Another direction for improvement would be to use a finer SoC discretization for the initial and final conditions of the optimization problem on each road segment for expected consumption calculation, as the error analysis has shown that the values of the discretized problem approximate the one of the original problem up to the order of the discretization step size.

Appendix A. VEHICLE MODEL

Neglecting the slope effect, for a given speed v and acceleration a, we can express the torque and rotation speed at the wheel as:

$$T_w(v(t), a(t)) = (ma(t) + \alpha_2 v^2(t) + \alpha_1 v(t) + \alpha_0) r_w$$
$$\omega_w(v, a) = \frac{60v}{2\pi r_w}$$

with m the vehicle mass, r_w the wheel radius, and $\alpha_0, \alpha_1, \alpha_2$ defining a quadratic approximation of the road-load force. We note G^i_R,G^i_{Eff},Pa_{ratio}, Pa_{eff} the ratio and efficiency for the gears and powertrain, and R the motor/engine reduction ratio. Then we get the torque at the primary shaft T_{prim} and the rotation speed of the engine ω_e and motor ω_m:

$$T_{prim}(v, a) = \max\left(\frac{T_w(v, a)}{Pa_{ratio} Pa_{eff} G^i_R G^i_{Eff}}, T_{min}\right)$$
$$\omega_e(v, a) = \omega_w(v, a) Pa_{ratio} G^i_R G^i_{Eff}$$
$$\omega_m(v, a) = \omega_w(v, a) Pa_{ratio} G^i_R G^i_{Eff} R$$

Table A.1. Parameters used in simulations

m	r_w	α_0	α_1	α_2
$1190kg$	0.31725m	113.5	0.774	0.4212

i	1	2	3	4	5
G^i_R	3.416	1.809	1.281	0.975	0.767
G^i_{Eff}	1	1	1	1	1

Pa_{ratio}	Pa_{eff}	R	$C_{max}(C)$
59/13	0.95	3.3077	5335200

REFERENCES

Ahn, K. and Rakha, H. (2007). Field evaluation of energy and environmental impacts of driver route choice decisions. In *2007 IEEE Intelligent Transportation Systems Conference*, 730–735.

Barth, M., Boriboonsomsin, K., and Vu, A. (2007). Environmentally-friendly navigation. In *2007 IEEE Intelligent Transportation Systems Conference*, 684–689.

Bellman, R. (1958). On a routing problem. *Quarterly of Applied Mathematics*, 16, 87–90.

Chau, K.T. and Wong, Y.S. (2002). Overview of power management in hybrid electric vehicles. *Energy Conversion and Management*, 43(15), 1953–1968.

Cormen, T.H. (2009). *Introduction to algorithms*. MIT press.

De Nunzio, G., Thibault, L., and Sciarretta, A. (2017). Model-based eco-routing strategy for electric vehicles in large urban networks. In *Comprehensive Energy Management–Eco Routing & Velocity Profiles*, 81–99. Springer.

Ericsson, E., Larsson, H., and Brundell-Freij, K. (2006). Optimizing route choice for lowest fuel consumption–potential effects of a new driver support tool. *Transportation Research Part C: Emerging Technologies*, 14(6), 369–383.

Le Rhun, A., Bonnans, F., De Nunzio, G., Leroy, T., and Martinon, P. (2019a). A bi-level energy management strategy for HEVs under probabilistic traffic conditions.

Le Rhun, A., Bonnans, F., De Nunzio, G., Leroy, T., and Martinon, P. (2019b). A stochastic data-based traffic model applied to vehicles energy consumption estimation. *IEEE Transactions on Intelligent Transportation Systems*, 1–10.

Lighthill, M.J. and Whitham, G.B. (1955). On kinematic waves. ii. a theory of traffic flow on long crowded roads. *Proceedings of the Royal Society of London. Series A, Mathematical and Physical Sciences*, 317–345.

Martelli, A. (1977). On the complexity of admissible search algorithms. *Artificial Intelligence*, 8(1), 1–13.

Nilsson, N.J. (1980). *Principles of artificial intelligence*. Tioga Publishing Co., Palo Alto, Calif.

Panwai, S. and Dia, H. (2005). Comparative evaluation of microscopic car-following behavior. *IEEE Transactions on Intelligent Transportation Systems*, 6(3), 314–325.